Talanta 134 (2015) 501–507

Contents lists available at ScienceDirect

Talanta

journal homepage: www.elsevier.com/locate/talanta

Doxorubicin-tethered fluorescent silica nanoparticles for pH-responsive anticancer drug delivery

Peng Zhang, Jilie Kong *

Department of Chemistry and Institutes of Biomedical Sciences, Fudan University, Shanghai, 200433, China

ARTICLE INFO

Article history:
Received 22 August 2014
Received in revised form
19 September 2014
Accepted 28 September 2014
Available online 29 October 2014

Keywords:
Doxorubicin
Fluorescent silica nanoparticle
Hydrazone
Drug delivery
Cancer therapy

ABSTRACT

The therapeutic potential of doxorubicin hydrochloride (DOX), an anticancer drug, is limited by its dose-related side effects and non-selective delivery to healthy and cancerous cells. Here we show a drug delivery system based on doxorubicin-tethered fluorescent silica nanoparticles (DOX-Hyd@FSiNPs). The DOX was conjugated to the FSiNPs through a hydrazone linkage. After uptake into the acidic environment of cancer cells, DOX was released from the FSiNPs' surfaces because of the breakage of the pH-sensitive hydrazine bond. The decreased viability of cells in the HeLa cancer cell line indicates that DOX-Hyd@FSiNPs are potential candidates for cancer therapy. Nuclear staining and Z-axis scanning with confocal laser scanning microscopy demonstrated that DOX-Hyd@FSiNPs were effectively delivered into the cytoplasm of HeLa cells; the released DOX accumulating in the nucleus. The fluorescence of the FSiNPs also allowed the live-tracking of the nanoparticles in the cell.

1. Introduction

Chemotherapy is commonly used to treat malignant cells; however, their therapeutic potential is limited by dose-related side effects, in part caused by their indiscriminant delivery to healthy and cancerous cells. Nanomaterials have emerged as potential drug carriers to help overcome these challenges; their small size (*i.e.*, below 100 nm) facilitating the accumulation of drugs in tumors through exploitation of the enhanced permeability and retention (EPR) effect [1]. There are various nanocarriers reported for use as drug delivery vehicles, such as mesoporous nanoparticles [2,3], gold nanoparticles [4–7], carbon nanotubes [8–10] and magnetic nanoparticles [11–13]. Silica nanoparticles (SiNPs) have emerged as excellent candidates for drug delivery because of their highly stability, good biocompatibility, large surface areas and the ease of surface modification [14–16].

Compared with traditional organic fluorescent dyes, dye-doped fluorescent silica nanoparticles FSiNPs are much brighter and more photostable [17], and have been used to detect nucleic acids [18,19] and image cells [20–22]. Furthermore, TAMRA-doped silica nanoparticles have been shown to selectively accumulate in the lysosomes of HeLa, MCF-7, MEAR and MSC cancer cells, and could be detected up to 30 times longer than LysoTracker Green, the standard dye for lysosome tracking.

Stimuli-responsive controlled release systems have been reported using redox [23–30], pH [31–36], and light [37–40] as triggers. The pH of tumor microenvironments and intracellular lysosomal compartments is more acidic than normal cells. Here we exploit this difference and design a pH responsive release system by conjugating DOX to FSiNPs through an acid-labile hydrazone linker [41–43] (Fig. 1A), the fluorescent properties allowing the nanoparticles to be tracked inside the cell. *In vitro* experiments showed that the DOX can be effectively released from doxorubicin-tethered fluorescent silica nanoparticles (DOX-Hyd@FSiNPs) in acidic environment. After cellular uptake (Fig. 1B), the viability of HeLa cells was reduced successfully.

2. Materials and methods

2.1. Materials

Tetraethylorthosilicate (TEOS), aminopropyltriethoxysilane (APTES), fluorescein isothiocyanate (FITC), 1-(3-Dimethylaminopropyl)-3-ethylcarbodiimide hydrochloride (EDC), N-Hydroxysulfosuccinimide (NHS) were purchased from Sigma-Aldrich (St. Louis, MO, USA). Carboxyethylsilanetriol Na salt (25% in water) was purchased from ABCR (Germany). Hydrazine monohydrate was purchased from Alfa Aesar China (Tianjin, China). Doxorubicin hydrochloride (DOX) was purchased from Beijing HuaFeng United Technology Co., Ltd.. 3-(4,5-dimethylthiazol-2-yl)-2,5-diphenyltetrazolium bromide (MTT) was purchased from Sangon Biotechnology Co., Ltd. (Shanghai, China).

* Corresponding author. Tel.: +86 21 65642138; fax: +86 21 65641740.
E-mail address: jlkong@fudan.edu.cn (J. Kong).

http://dx.doi.org/10.1016/j.talanta.2014.09.041
0039-9140/

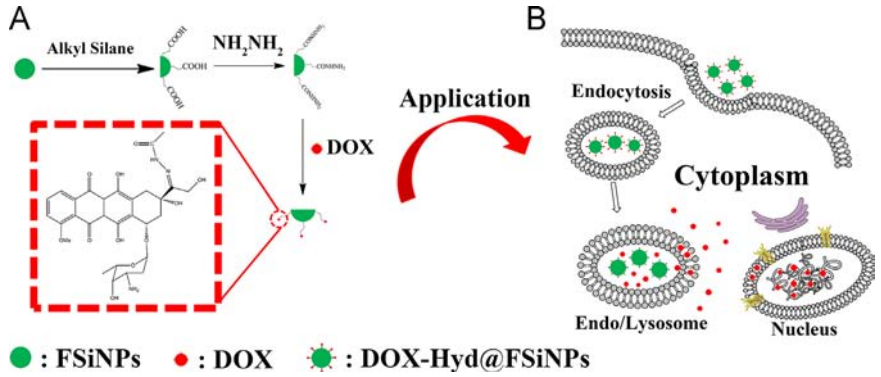

Fig. 1. (A) Schematic of synthesis of DOX-Hyd@FSiNPs and (B) After endocytotic uptake, the pH-responsive release of DOX inside the acidic cellular environment of a cancer cell.

Dulbecco's Modified Eagle's Medium (DMEM), fetal calf serum (FCS) were purchased from GBICO. 2-(4-amidinophenyl)-6-indolecarbamidine dihydrochloride (DAPI) was purchased from KeyGen Biotech. (Nanjing, China). All reagents and solvents were of analytical grade and used as received.

2.2. Synthesis of FITC-doped silica nanoparticles and carboxylic acid modified FSiNPs

FITC (1 mg) was dissolved in n-hexanol (1 mL) under sonication. APTES (10 μL) was added and the reaction mixture stirred magnetically for 24 h. Typically, FSiNPs were synthesized in a W/O microemulsion system consisting of a mixture of Triton X-100 (10.8 mL), n-hexanol (9.8 mL), cyclohexane (45.0 mL), deionized water (3.0 mL), FITC-APTES solution (1.0 mL) and TEOS (0.6 mL), which was stirred for 30 min, before ammonium hydroxide (0.60 mL) was added. After 24 h of stirring, FSiNPs were isolated from the microemulsion with acetone followed by several centrifugation and washing steps with ethanol and water to remove the surfactant and the impurities. The FSiNPs obtained were dispersed in water (10 mL), followed by the addition of acetic acid (100 μL, 0.1 M) and carboxyethylsilanetriol Na salt (200 μL) and stirred for 24 h. Finally, carboxylic acid-modified FSiNPs (FSiNPs-COOH) were centrifuged and washed with water for several times. Purified FSiNPs-COOHs were stored in water until further use.

2.3. Synthesis of doxorubicin-tethered FSiNPs

The above purified FSiNPs-COOH were diluted to 50 mL with H_2O, then, EDC (60 mg), NHS (20 mg) and hydrazine monohydrate (5 mL) were added into the above solution and stirred overnight. The precipitates were separated by centrifugation and washed several times with deionized water to yield the hydrazine modified FSiNPs nanocomposites (hydrazine@FSiNPs). Thirty mg of hydrazine@FSiNPs were dispersed in 5 mL of methanol and 6 mg of DOX added to the above solution, which was stirred at room temperature for 48 h. The precipitates were separated by centrifugation and washed with methanol several times until the supernatant became colorless. DOX-conjugated FSiNPs (DOX-Hyd@FSiNPs) were dried under vacuum. All of the supernatants were collected and diluted to 100 mL with methanol in a volumetric flask for evaluation of drug-loading efficiency by UV–vis spectroscopy.

2.4. In vitro DOX release

Two batches of DOX-Hyd@FSiNPs (10 mg) were suspended in 4 mL of PBS buffer with pH values of 7.4 and 5.5. The suspensions were transferred into dialysis bag (MW = 14000), and placed into a beaker containing 100 mL of PBS buffer with the same pH conditions. At a fixed timed point, 1 mL of solution was withdrawn from the beaker and analyzed by UV–vis spectroscopy.

2.5. Cell culture

Human cervical carcinoma (HeLa) cells were routinely cultured at 37 °C in flasks containing Dulbecco's Modified Eagle Medium (DMEM) with 10% fetal calf serum (FCS) in a humidified atmosphere and with 5% CO2 in a Thermo culturist.

2.6. Cytotoxicity assay

The cytotoxicity of Hydrazine@FSiNPs and DOX-Hyd@FSiNPs' cytotoxicity was determined by MTT assay. HeLa cells were first seeded at 10^4 per cell into the 96-well cell culture plate in DMEM with 10% FCS at 37 °C and with 5% CO_2 for 24 h. Different concentrations of nanoparticles were then added. After incubation for 24 h, MTT (100 μL, 5 mg/mL) was added and incubated for a further 4 h. Finally, the formed formazan was dissolved in DMSO. The absorbance at 492 nm was recorded by an automatic ELISA analyzer (SPR-960).

2.7. Cellular internalization and localization

HeLa cells were grown in DMEM supplemented with 10% FCS at 37 °C and 5% CO_2. Cells were seeded on 15 mm glass bottom petri dishes and allowed to adhere for 24 h, followed by washing with PBS three times. The adhered cells were incubated with DOX-Hyd@FSiNPs in DMEM-10% FCS for a fixed time at 37 °C under 5% CO_2 and then fixed with 4% paraformaldehyde in PBS for 15 min and stained with DAPI (0.2 μg / mL) in PBS for 20 min at 37 °C. Confocal fluorescence imaging was performed with a Leica laser scanning confocal microscope (Leica TCS SP5) and a 40 × objective lens.

3. Results and discussion

3.1. Synthesis and characterization of DOX-Hyd@FSiNPs

The synthesis of FSiNPs was achieved by a microemulsion method [20]. Carboxyethylsilanetriol Na salt (25% in water) was added to FSiNPs solution under acidic conditions resulting in the carboxyl group covalently linked to the surface of the nanoparticle. Hydrazine monohydrate was then reacted with carboxyl group with the help of EDC and NHS to form an active ester. Finally, a hydrazone bond was formed between the ketone group of DOX and the

hydrazine group. The as-prepared FSiNPs had good uniformity and monodispersity, with an average diameter of 50 nm as measured by transmission electron microscopy (Fig. 2A). Photoluminescence analyses showed that the fluorescein dye had been doped into silica nanoparticles (Fig. 2B). As FITC was covalently linked to the silica matrix, no dye leaking was observed in the aqueous supernatant upon centrifugation. The hydrodynamic diameter of FSiNPs in water was measured by dynamic light scattering (DLS), and showed an average diameter of 117.3 nm with relatively narrow distribution (polydispersity index (PDI)=0.107; Fig. 2C). The measured ζ-potential (−30 mV) indicated that the FSiNPs were stable (Fig. 2D).

The fluorescence emissions of FSiNPs were more intense when excited at 495 nm than those observed for DOX-Hyd@FSiNPs (Fig. 3A). This can be explained by the fluorescence resonance energy transfer (FRET) effect [11,44]; the fluorescence of FSiNPs quenched by conjugated DOX. Additionally, the spectra for DOX-Hyd@FSiNPs (Fig. 3B), revealed an additional absorption peak at 550 nm, characteristic of DOX.

FT-IR was used to study the surface modification process on FSiNPs (Fig. 4). Asymmetric and symmetric stretching vibrations of the methylene (CH_2) were observed at 2960 and 2848 cm^{-1}, respectively, inferring that the carboxyethylsilane agent was successfully added to

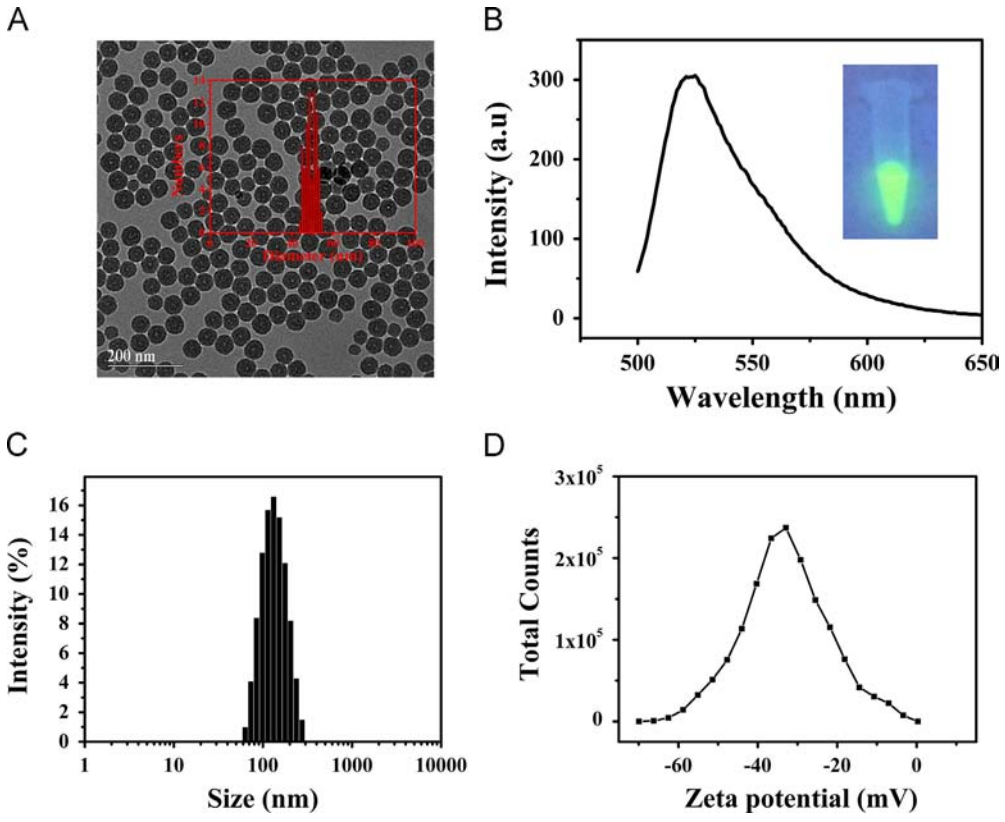

Fig. 2. (A) TEM images of FSiNPs. Inset: size distributions of the FSiNPs calculated from TEM images; (B) Fluorescence emission spectrum of FSiNPs. Inset: photograph of the fluorescence color of FSiNPs under a hand-held UV lamp, Excitation wavelength: 365 nm; (C) DLS and (D) zeta potential of FSiNPs.

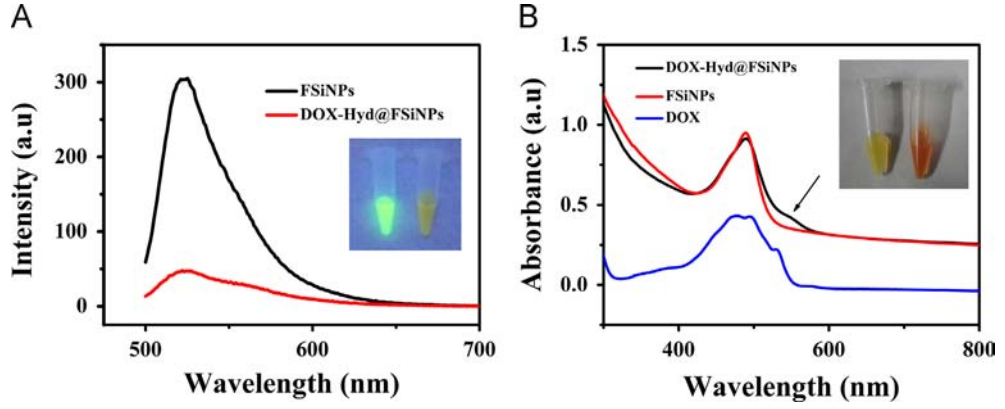

Fig. 3. (A) Fluorescence emission spectra of FSiNPs (black) and DOX-Hyd@FSiNPs (red), excitation wavelength: 495 nm, emission wavelength: 500–700 nm. Inset: photograph of the fluorescence color for FSiNPs (left) and DOX-Hyd@FSiNPs (right) under a hand-held UV lamp, excitation wavelength: 365 nm; (B) UV absorbance spectra of DOX (blue), FSiNPs (red) and DOX-Hyd@FSiNPs (black), the arrow indicated the characteristic UV absorption of DOX. Inset: photograph of FSiNPs (left) and DOX-Hyd@FSiNPs (right) under daylight.

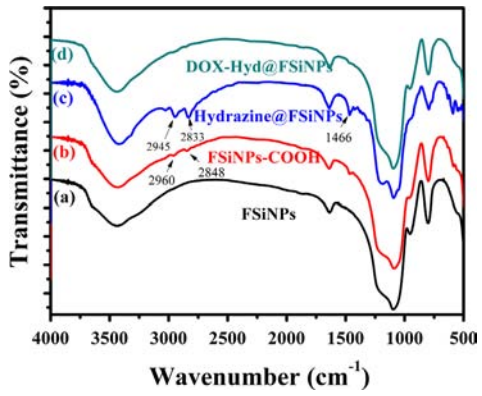

Fig. 4. FT-IR spectra of FSiNPs (a), carboxylic acid modified FSiNPs (b), hydrazine-modified FSiNPs (c) and DOX modified FSiNPs (d).

Table 1
DLS and Zeta of FSiNPs, carboxylic acid modified FSiNPs, hydrazine modified FSiNPs and DOX- tethered FSiNPs.

	DLS (nm)	Zeta Potential (mV)
FSiNPs	119.0 ± 4.3	−32.8 ± 1.1
FSiNPs-COOH	98.2 ± 6.8	−35.9 ± 3.9
Hydrazine@FSiNPs	107.3 ± 3.2	−20.5 ± 0.6
DOX-Hyd@FSiNPs	95.8 ± 5.9	−31.2 ± 2.9

The data were expressed as mean ± SEM ($n=3$)

the FSiNPs' surfaces. After conjugation with hydrazine, a new absorption peak was detected at 1466 cm^{-1} and could be attributed to the asymmetric stretching vibrations of an amino group (NH_2). These peaks were no longer observed on the addition of DOX, as expected.

Changes in DLS and zeta potential values also reflected the successive surface modifications (Table 1). From the DLS data, the surface modification appeared to be relatively moderate and did not affect the morphology of the original FSiNPs. Conversely, the values of zeta potential changed more obviously, particularly after the conjugation of hydrazine and DOX.

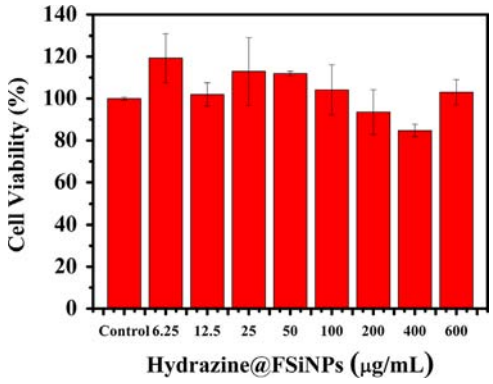

Fig. 5. Cell viability results after incubation of the HeLa cells with various concentrations of hydrazine@FSiNPs for 24 h. The data were expressed as mean ± SEM ($n=4$).

3.2. Controlled drug release and in vitro cytotoxicity

A standard MTT assay was used to evaluate the cytotoxicity (Fig. 5), and therefore, biocompatibility, of the hydrazine-modified FSiNPs (hydrazine@FSiNPs) toward HeLa cells. At concentrations of hydrazine@FSiNPs as high 600 μg/mL, the cell viability was around 100%, indicating that the hydrazine@FSiNPs nanocomposites were suitable as drug carriers.

Next, we examined the drug loading and *in vitro* release abilities of DOX-Hyd@FSiNPs. The loading of DOX onto the FSiNPs was reverse calculated from the unbound drug in solution and estimated to be around 32.67 μg/mg. DOX release from the nanoparticles in PBS buffer solutions with pH values of 7.4 and 5.5 were profiled (Fig. 6A). The drug release rate of DOX at pH 5.5 was much faster than at pH 7.4 and can be attributed to the cleavage of the hydrazone bond.

The cytotoxic effect of DOX-Hyd@FSiNPs in HeLa cells was evaluated. Both free DOX and DOX-Hyd@FSiNPs exhibited an increasing cytotoxicity against HeLa cells with increasing concentration (Fig. 6B). Around 52% of cells were no longer viable at the highest concentration of DOX-Hyd@FSiNPs. The cytotoxicity of DOX was slightly higher than that of DOX-Hyd@FSiNPs, (about 56.7%). This may be attributed to the partial release of DOX from DOX-Hyd@FSiNPs, where around 50% DOX was released after 24 h; longer studies may demonstrate the sustained release of the drug from the nanoparticles. As mentioned previously, nanoparticle drug delivery systems are shown to improve drug delivery through the EPR effect; therefore, the enhanced performance and benefits of the DOX-Hyd@FSiNPs may be more evident *in vivo* as opposed to the monolayer of cells used *in vitro* testing.

3.3. Tracking of cellular uptake

The pH-controlled drug release properties of DOX-Hyd@FSiNPs toward HeLa cells were investigated using CLSM. As shown in Fig. 7, red fluorescence, attributed to unbound DOX, was observed

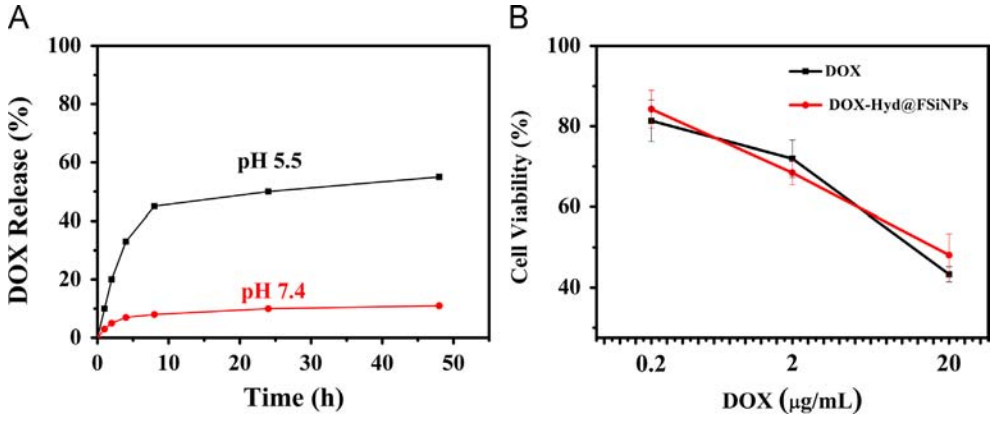

Fig. 6. (A) DOX release from DOX-Hyd@FSiNPs at pH 5.5 (black) and pH 7.4 (red) PBS buffer; (B) Cell viability results after incubation of the HeLa cells with three concentrations of DOX (black) and DOX-Hyd@FSiNPs (red) for 24 h.

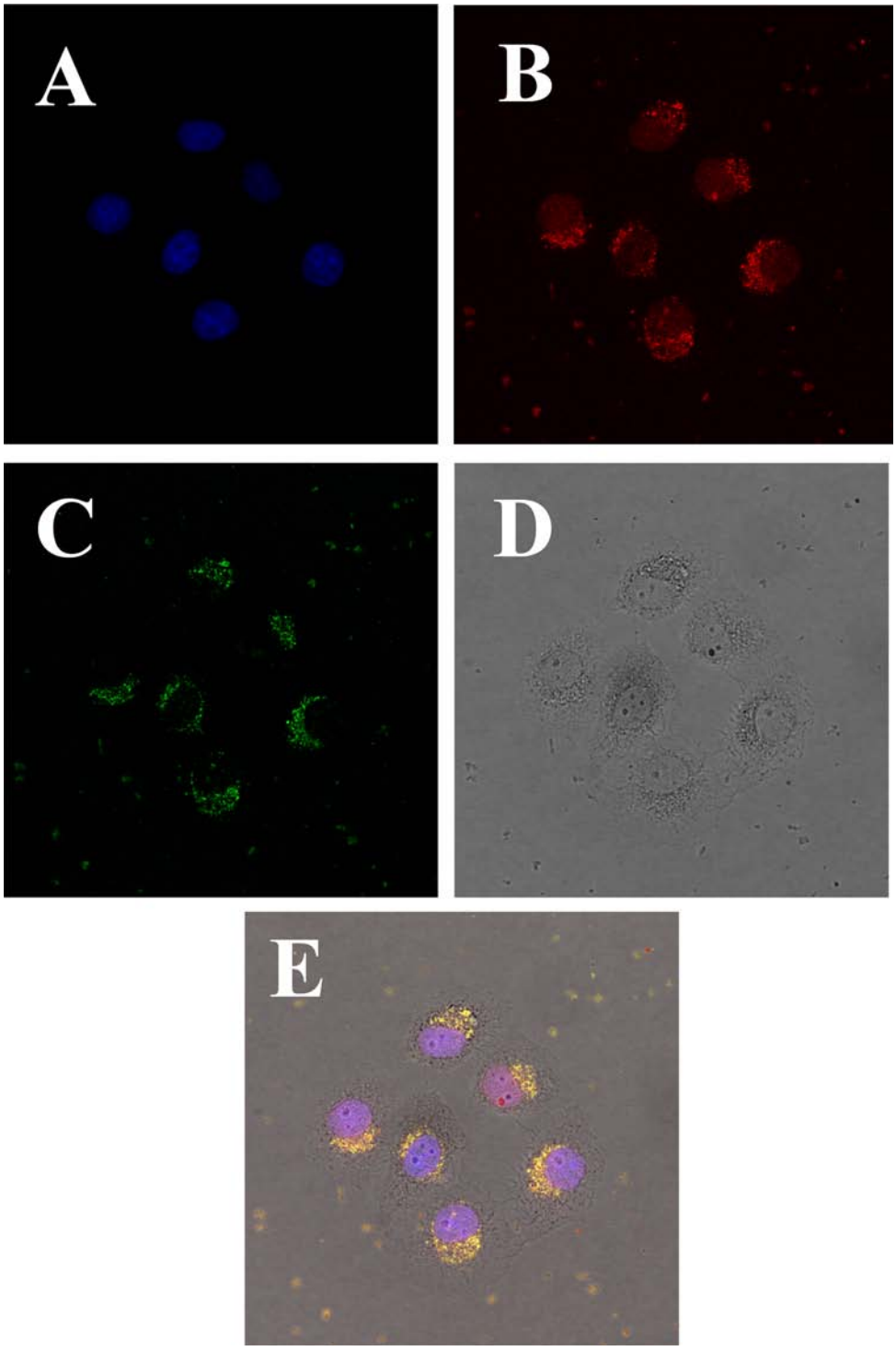

Fig. 7. Confocal microscopy fluorescence images of HeLa cells after incubation of DOX-Hyd@FSiNPs for 12 h. (A) nucleus fluorescence images (blue); (B) DOX fluorescence images (red); (C) FSiNPs fluorescence images (green); (D) bright field image; (E) merged image, the yellow is a result of overlap of green (FSiNPs) and red (DOX), the purple is the result of overlap of blue (DAPI) and red (DOX). The excitation wavelength of DAPI is 405 nm, emission collected from 450 to 480 nm (blue), excitation wavelength of DOX and FSiNPs is 488 nm, emission collected from 550 to 700 nm (red) and 500 to 530 nm (green), respectively.

not only in the cytoplasm, but also, as expected, in the nucleus, after being cultured with DOX-Hyd@FSiNPs for 12 h. DOX exerts is therapeutic effect by intercalating with double-stranded DNA in nucleus, thus inhibiting the activities of topoisomerase [45]. In agreement with previous studies, green fluorescence, associated with the fluorescence of the nanoparticles, was observed in the cytoplasm but not in the nucleus [46]. To further understand where DOX exerted its function, the intracellular location of DOX-Hyd@FSiNPs nanocomposites in a single cell was investigated by CLSM using line-plots fluorescent microscopy [47], revealing the spatial distribution of the DOX-Hyd@FSiNPs inside HeLa cells. As shown in Fig. 8, quantification of the luminescence intensity profile of DOX-Hyd@FSiNPs-treated cells revealed that, while most of the composites were located in the perinuclear regions where

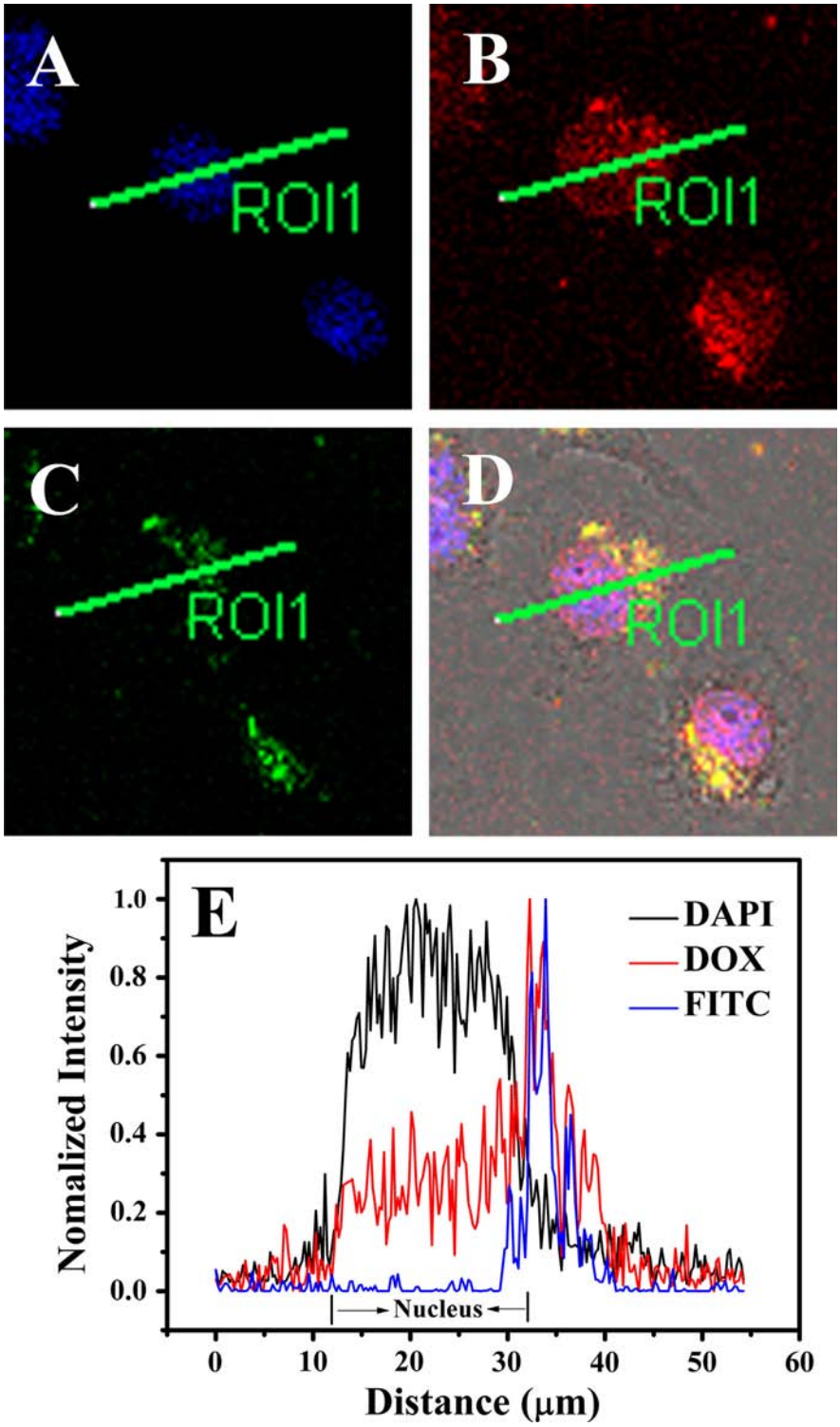

Fig. 8. Confocal microscopy fluorescence images and line-scanning profiles of fluorescence intensity for HeLa cells incubated for 12 h with DOX-Hyd@FSiNPs. (A) nucleus fluorescence images; (B) DOX fluorescence images; (C) FSiNPs fluorescence images; (D) merged images; (E) Line-scanning profiles of luminescence intensity in confocal fluorescence images. [FSiNPs]=40 μg/mL.

endosomes existed, only the unbound DOX diffused into the nucleus. Z-axis fluorescent microscopy (Figs. S1–5 and Video S1) further confirmed the position of the nanocomposites.

Supplementary material related to this article can be found online at http://dx.doi.org/10.1016/j.talanta.2014.09.041.

4. Conclusions

In summary, we have successfully developed a FSiNPs-based pH-controlled drug delivery and release system. The DOX was chemically conjugated to the FSiNPs through a pH-sensitive hydrazone linkage.

After endocytosis, the DOX released from the FSiNPs because of the acidic environment inside cancer cells. *In vitro* assays demonstrated that the Hydrazine@FSiNPs nanocomposites themselves have good biocompatibilities; however, after loading with DOX, they have shown similar killing efficiency compared with the free drug.

Acknowledgment

This work was supported by the National Natural Science Foundation of China (21175029 and 21335002).

Appendix A. Supporting information

Supplementary data associated with this article can be found in the online version at http://dx.doi.org/10.1016/j.talanta.2014.09.041.

References

[1] Y. Matsumura, H. Maeda, Cancer Res. 46 (1986) 6387–6392.
[2] M. Vallet-Regi, A. Ramila, R.P. del Real, J. Perez-Pariente, Chem. Mater. 13 (2001) 308–311.
[3] J. Lu, M. Liong, Z.X. Li, J.I. Zink, F. Tamanoi, Small 6 (2010) 1794–1805.
[4] S. Aryal, J.J. Grailer, S. Pilla, D.A. Steeber, S.Q. Gong, J. Mater. Chem. 19 (2009) 7879–7884.
[5] Y.L. Luo, Y.S. Shiao, Y.F. Huang, ACS Nano 5 (2011) 7796–7804.
[6] M. Prabaharan, J.J. Grailer, S. Pilla, D.A. Steeber, S.Q. Gong, Biomaterials 30 (2009) 6065–6075.
[7] F. Wang, Y.C. Wang, S. Dou, M.H. Xiong, T.M. Sun, J. Wang, ACS Nano 5 (2011) 3679–3692.
[8] R.B. Li, R. Wu, L. Zhao, M.H. Wu, L. Yang, H.F. Zou, ACS Nano 4 (2010) 1399–1408.
[9] Z. Liu, A.C. Fan, K. Rakhra, S. Sherlock, A. Goodwin, X.Y. Chen, Q.W. Yang, D.W. Felsher, H.J. Dai, Angew. Chem. Int. Ed. 48 (2009) 7668–7672.
[10] Z. Liu, X.M. Sun, N. Nakayama-Ratchford, H.J. Dai, ACS Nano 1 (2007) 50–56.
[11] S.S. Banerjee, D.H. Chen, Nanotechnology 19 (2008) 505104.
[12] M.K. Yu, J. Park, Y.Y. Jeong, W.K. Moon, S. Jon, Nanotechnology 21 (2010) 415102.
[13] Z.H. Zhao, D.T. Huang, Z.Y. Yin, X.Q. Chi, X.M. Wang, J.H. Gao, J. Mater. Chem. 22 (2012) 15717–15725.
[14] C.A. Barnes, A. Elsaesser, J. Arkusz, A. Smok, J. Palus, A. Lesniak, A. Salvati, J.P. Hanrahan, W.H. de Jong, E. Dziubaltowska, M. Stepnik, K. Rydzynski, G. McKerr, I. Lynch, K.A. Dawson, C.V. Howard, Nano Lett. 8 (2008) 3069–3074.
[15] L.C.J. Thomassen, A. Aerts, V. Rabolli, D. Lison, L. Gonzalez, M. Kirsch-Volders, D. Napierska, P.H. Hoet, C.E.A. Kirschhock, J.A. Martens, Langmuir 26 (2010) 328–335.
[16] T. Yu, A. Malugin, H. Ghandehari, ACS Nano 5 (2011) 5717–5728.
[17] X.J. Zhao, R.P. Bagwe, W.H. Tan, Adv. Mater. 16 (2004) 173–176.
[18] X.J. Zhao, R. Tapec-Dytioco, W.H. Tan, J. Am. Chem. Soc. 125 (2003) 11474–11475.
[19] L. Wang, C. Lofton, M. Popp, W. Tan, Bioconjugate Chem 18 (2007) 610–613.
[20] S. Santra, H. Yang, D. Dutta, J.T. Stanley, P.H. Holloway, W.H. Tan, B.M. Moudgil, R.A. Mericle, Chem. Commun. (2004) 2810–2811.
[21] S. Santra, B. Liesenfeld, D. Dutta, D. Chatel, C.D. Batich, W.H. Tan, B.M. Moudgil, R.A. Mericle, J. Nanosci. Nanotechnol. 5 (2005) 899–904.
[22] H. Shi, X.X. He, Y. Yuan, K.M. Wang, D. Liu, Anal. Chem. 82 (2010) 2213–2220.
[23] S. Giri, B.G. Trewyn, M.P. Stellmaker, V.S.Y. Lin, Angew. Chem. Int. Ed. 44 (2005) 5038–5044.
[24] R. Hernandez, H.R. Tseng, J.W. Wong, J.F. Stoddart, J.I. Zink, J. Am. Chem. Soc. 126 (2004) 3370–3371.
[25] H. Kim, S. Kim, C. Park, H. Lee, H.J. Park, C. Kim, Adv. Mater. 22 (2010) 4280–4283.
[26] C.Y. Lai, B.G. Trewyn, D.M. Jeftinija, K. Jeftinija, S. Xu, S. Jeftinija, V.S.Y. Lin, J. Am. Chem. Soc. 125 (2003) 4451–4459.
[27] R. Liu, X. Zhao, T. Wu, P.Y. Feng, J. Am. Chem. Soc. 130 (2008) 14418–14419.
[28] Z. Luo, K.Y. Cai, Y. Hu, L. Zhao, P. Liu, L. Duan, W.H. Yang, Angew. Chem. Int. Ed. 50 (2011) 640–643.
[29] T.D. Nguyen, Y. Liu, S. Saha, K.C.F. Leung, J.F. Stoddart, J.I. Zink, J. Am. Chem. Soc. 129 (2007) 626–634.
[30] T.D. Nguyen, H.R. Tseng, P.C. Celestre, A.H. Flood, Y. Liu, J.F. Stoddart, J.I. Zink, Proc. Natl., Acad. Sci. U. S. A 102 (2005) 10029–10034.
[31] E. Aznar, M.D. Marcos, R. Martinez-Manez, F. Sancenon, J. Soto, P. Amoros, C. Guillem, J. Am. Chem. Soc. 131 (2009) 6833–6843.
[32] S. Bhattacharyya, H.S. Wang, P. Ducheyne, Acta Biomater. 8 (2012) 3429–3435.
[33] R. Casasus, E. Climent, M.D. Marcos, R. Martinez-Manez, F. Sancenon, J. Soto, P. Amoros, J. Cano, E. Ruiz, J. Am. Chem. Soc. 130 (2008) 1903–1917.
[34] T.D. Nguyen, K.C.F. Leung, M. Liong, C.D. Pentecost, J.F. Stoddart, J.I. Zink, Org. Lett. 8 (2006) 3363–3366.
[35] C. Park, K. Oh, S.C. Lee, C. Kim, Angew. Chem. Int. Ed. 46 (2007) 1455–1457.
[36] S. Angelos, Y.W. Yang, K. Patel, J.F. Stoddart, J.I. Zink, Angew. Chem. Int. Ed. 47 (2008) 2222–2226.
[37] D.P. Ferris, Y.L. Zhao, N.M. Khashab, H.A. Khatib, J.F. Stoddart, J.I. Zink, J. Am. Chem. Soc. 131 (2009) 1686–1688.
[38] N.K. Mal, M. Fujiwara, Y. Tanaka, Nature 421 (2003) 350–353.
[39] J.L. Vivero-Escoto, C.W. Slowing II, V.S.Y. Wu, Lin, J. Am. Chem. Soc. 131 (2009) 3462–3463.
[40] Q. Yuan, Y.F. Zhang, T. Chen, D.Q. Lu, Z.L. Zhao, X.B. Zhang, Z.X. Li, C.H. Yan, W.H. Tan, ACS Nano 6 (2012) 6337–6344.
[41] X. Ding, Y. Liu, J. Li, Z. Luo, Y. Hu, B. Zhang, J. Liu, J. Zhou, K. Cai, ACS Appl. Mater. Interfac. 6 (2014) 7395–7407.
[42] T. Etrych, V. Subr, R. Laga, B. Rihova, K. Ulbrich, Eur. J. Pharm. Sci. 58 (2014) 1–12.
[43] M. Dickerson, N. Winquist, Y. Bae, Pharm. Res. 31 (2014) 1254–1263.
[44] V. Bagalkot, L. Zhang, E. Levy-Nissenbaum, S. Jon, P.W. Kantoff, R. Langer, O.C. Farokhzad, Nano Lett. 7 (2007) 3065–3070.
[45] S.Y. Han, Y.X. Liu, X. Nie, Q. Xu, F. Jiao, W. Li, Y.L. Zhao, Y. Wu, C.Y. Chen, Small 8 (2012) 1596–1606.
[46] L.M. Pan, Q.J. He, J.N. Liu, Y. Chen, M. Ma, L.L. Zhang, J.L. Shi, J. Am. Chem. Soc. 134 (2012) 5722–5725.
[47] C.Y. Li, M.X. Yu, Y. Sun, Y.Q. Wu, C.H. Huang, F.Y. Li, J. Am. Chem. Soc. 133 (2011) 11231–11239.